**Electronic Supplementary Information (ESI)**

# Novel Green Phosphorescence from Pristine ZnO Quantum Dot: Tuning of Correlated Color Temperature

[1]Sensor and Actuator Division, CSIR- Central Glass and Ceramic Research Institute, Kolkata-700032, West Bengal, India

**Corresponding authors e-mail ID: palm@cgcri.res.in

[2]School of Nanoscience and Technology, Jadavpur University, Kolkata- 700032, West Bengal, India

*Corresponding authors e-mail ID: chandu_ju@yahoo.co.in

[3]Department of Metallurgical and Material Engineering, Jadavpur University, West Bengal, India

**S-1**: TEM Images of (a) ZCF1, (b) ZCF2, (c) ZNC and their respective FFT plots in the inset

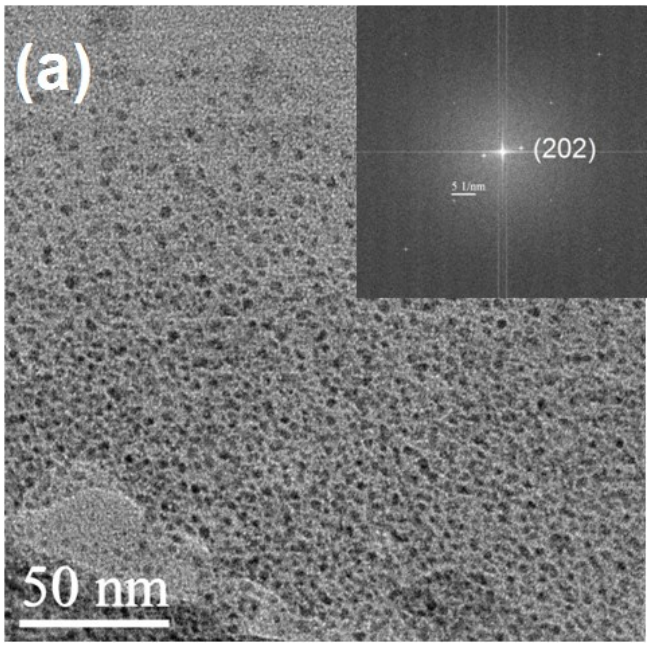


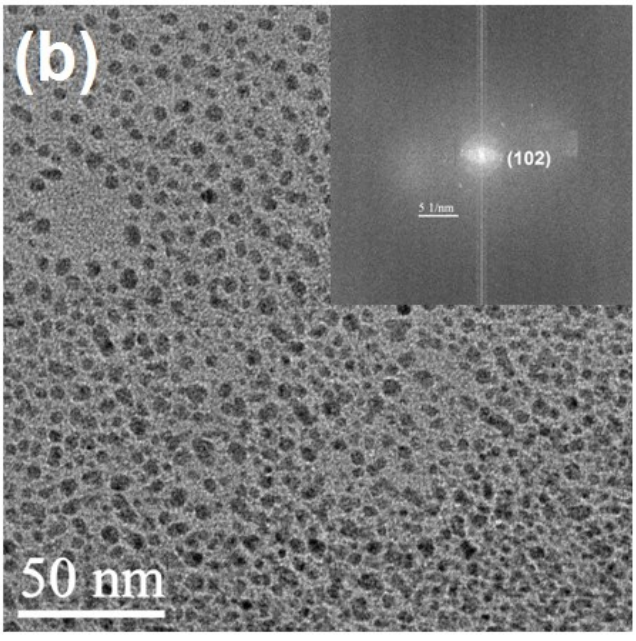

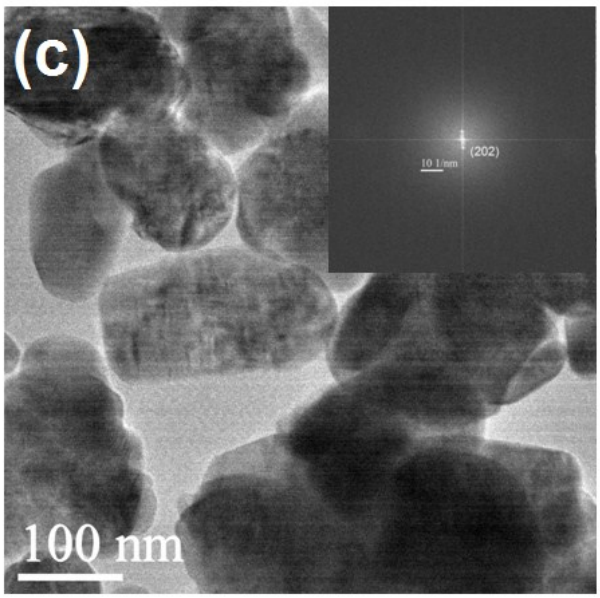
(c)
(202)
10 1/nm
100 nm

**S-2**: Particle Size Distribution Plots of (a) ZQD [mean particle diameter 5.38+-0.87 nm], (b) ZCF1 [mean particle diameter 5.41+-0.39 nm], (c) ZCF2 [mean particle diameter 5.56 +-0.47 nm]

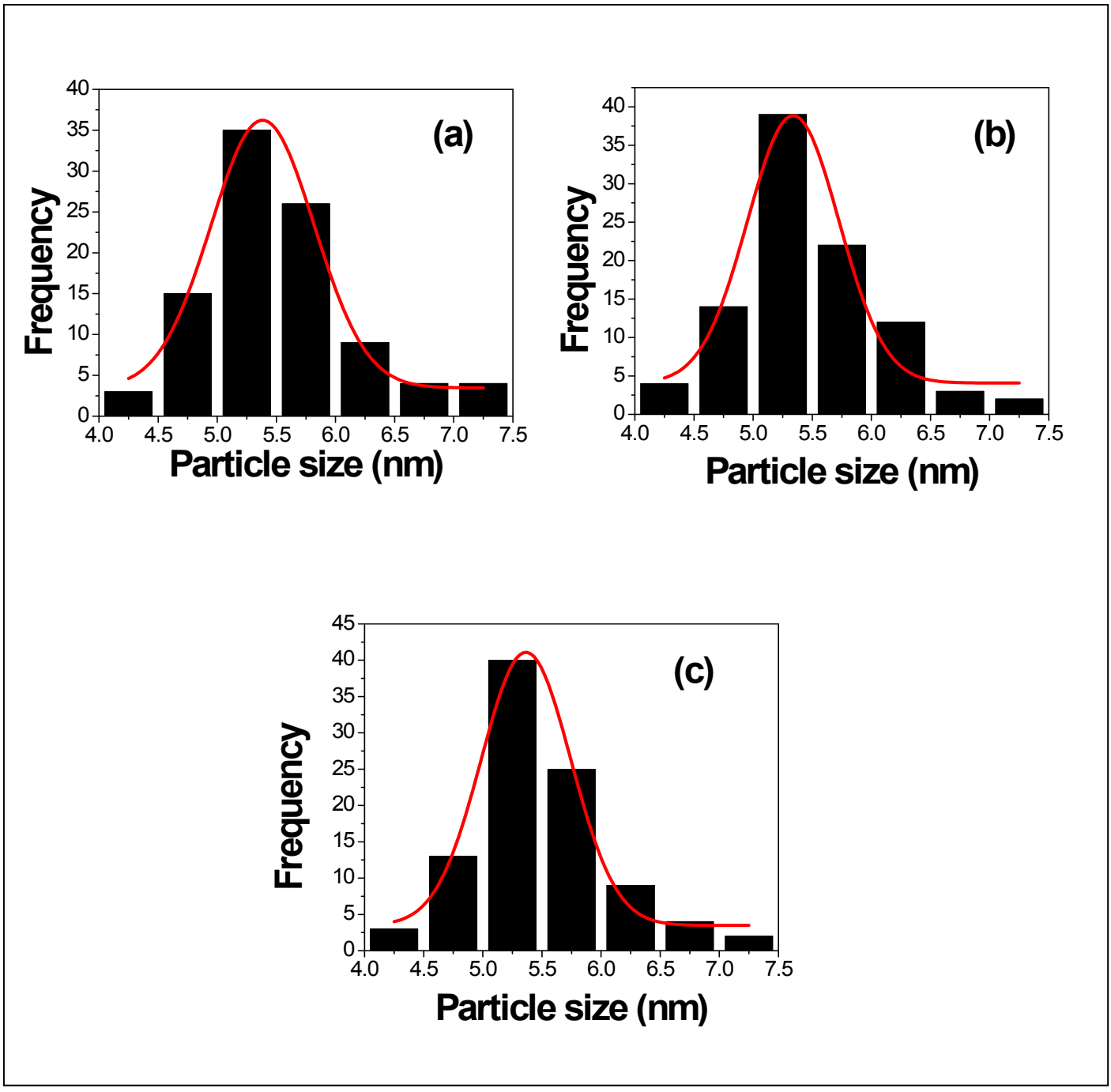

**S-3**: Raman Spectra of (a) ZNC, (b) ZQD, (c) ZCF1, (d) ZCF2

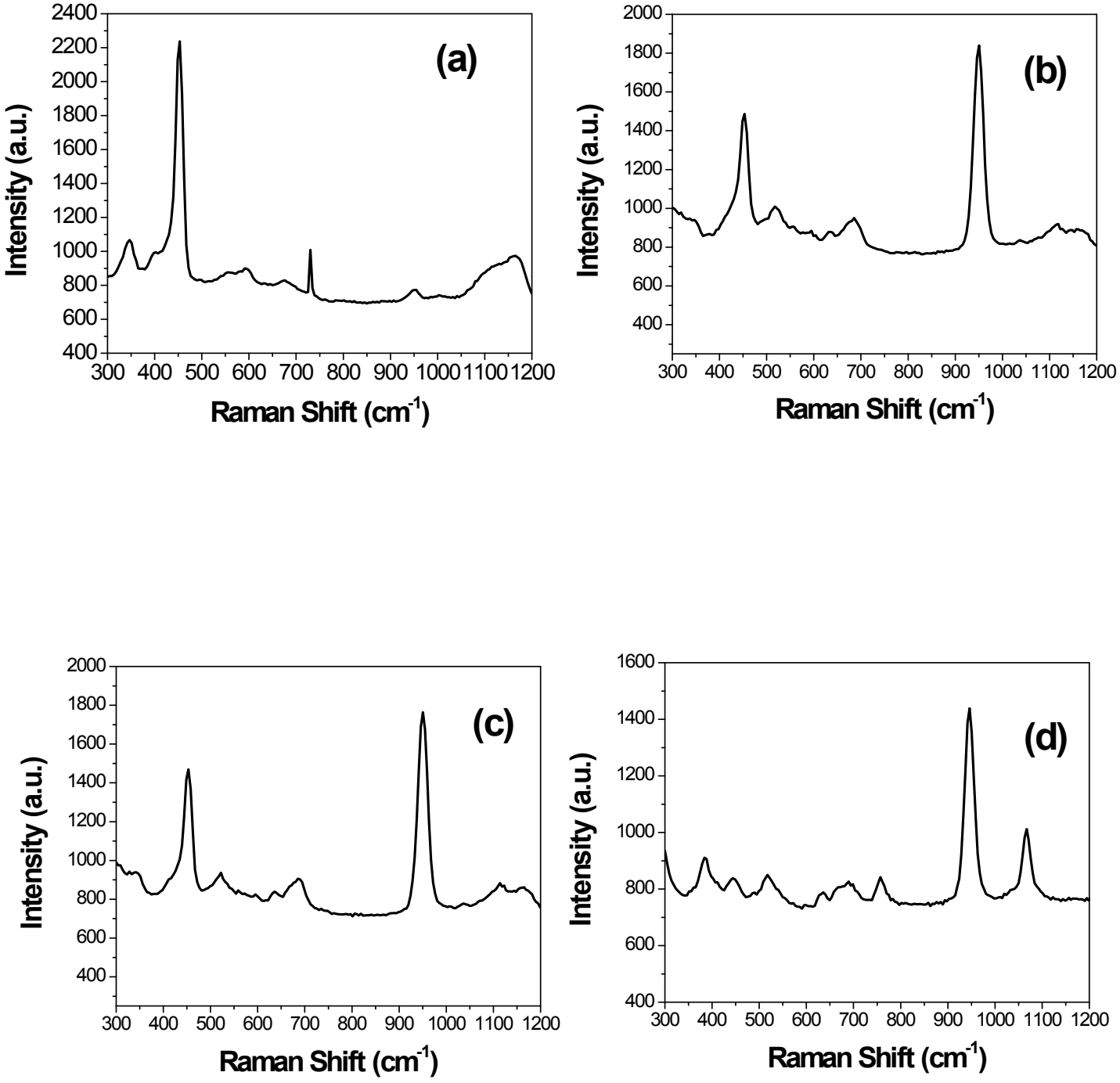

**S-4**: Raman peaks detected in the Spectrums of ZNC, ZQD, ZCF1 and ZCF2

| ZQD ($nm^{-1}$) | Assignment | ZCF1 ($nm^{-1}$) | Assignment | ZCF2 ($nm^{-1}$) | Assignment | ZNC ($nm^{-1}$) | Assignment |
|---|---|---|---|---|---|---|---|
| 345 | $E_2$(high)- $E_2$(low) | 345 | $E_2$(high)- $E_2$(low) | 384 | $E_2$(high)- $E_2$(low) | 345 | $E_2$(high)- $E_2$(low) |
| - | - | - | - | | | 400 | $A_1$(TO) |
| 451 | Oxygen sublattice $A_1$(LO) mode | 451 | Oxygen sublattice $A_1$(LO) mode | 444 | Oxygen sublattice $A_1$(LO) mode | 451 | Non-polar vibrational mode of oxygen sublattice with $E_2$ symmetry, fingerprint of wurzite crystal structure of ZnO. |
| 518 | Surface phonon mode | 518 | Surface phonon mode | 518 | Surface phonon mode | - | - |
| - | - | - | - | -- | - | 558 | Surface phonon |
| 583 | $A_1$(LO) | 583 | $A_1$(LO) | - | - | 593 | $A_1$(LO) |
| 685 | Oxygen sublattice TA+LO mode | 685 | Oxygen sublattice TA+LO mode | 685 | TA+LO phonon mode | 685 | TA+LO phonon mode |
| - | - | - | - | - | - | 729 | Second order $E_{2L}$-$B_{1H}$ phonon mode |
| 1116 | $A_1$(2LO) | 1116 | $A_1$(2LO) | - | - | 1164 | $A_1$(2LO) |

**S-5**: Near band gap PL emissions of ZQD, ZCF1, ZCF2, ZNC, ZNC2 powders excited at 4.1 eV.

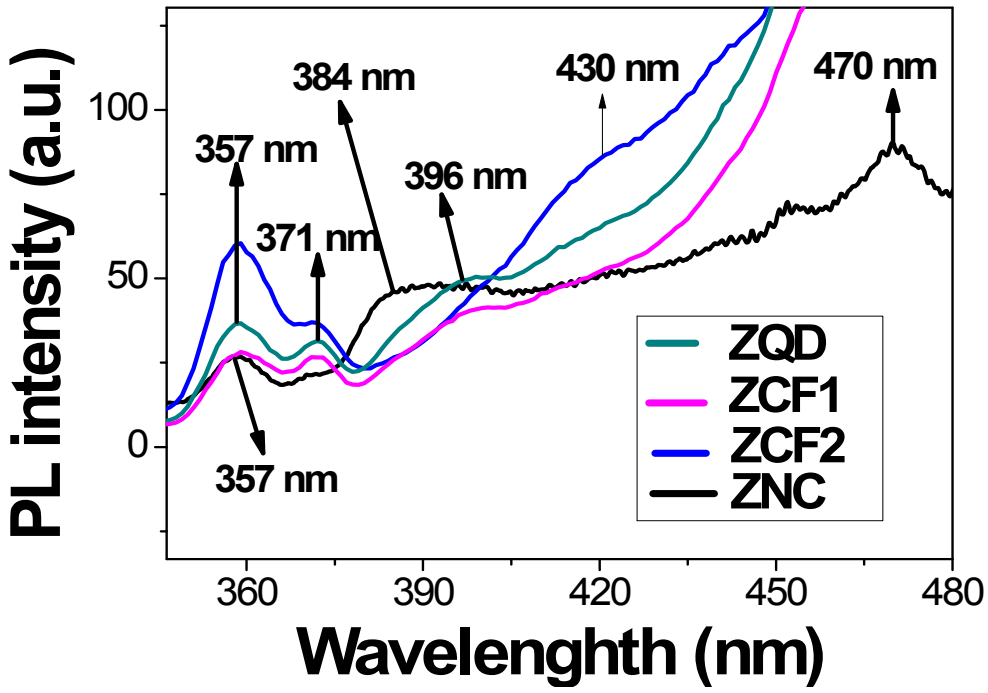


**S-6**: EPR plot of ZQD, ZCF1, ZCF2, ZNC

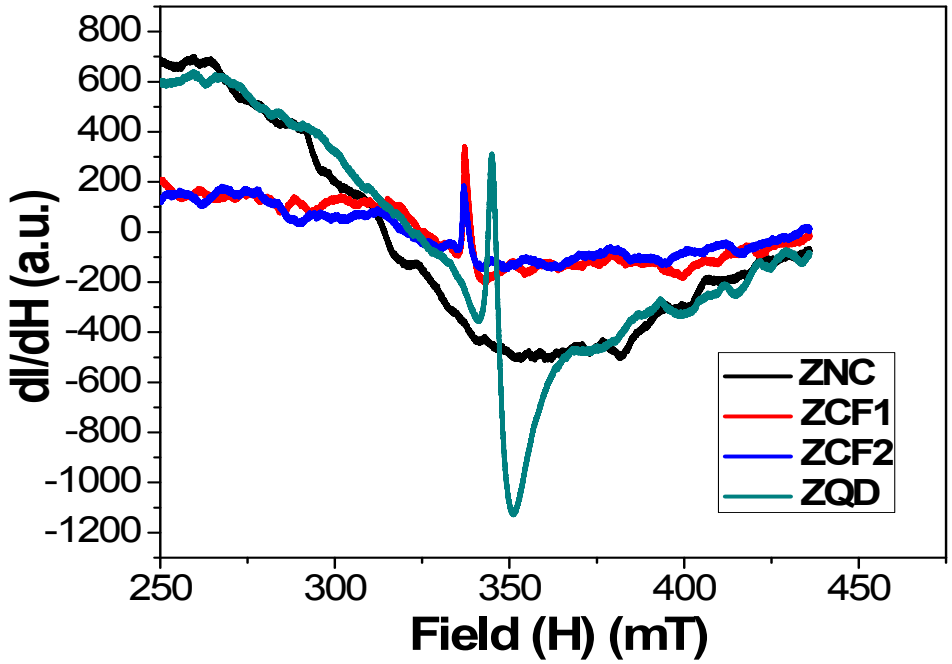

S-7: **(A)** PL emissions plots of (a) ZQD, (b)ZCF1 and (c)ZCF2 fitted by Gaussian curve. In all cases the PL emission plots can be deconvoluted into two Gaussian curves: one peaked in the UV range and another peaked at 545 nm signifying green luminescence**.**

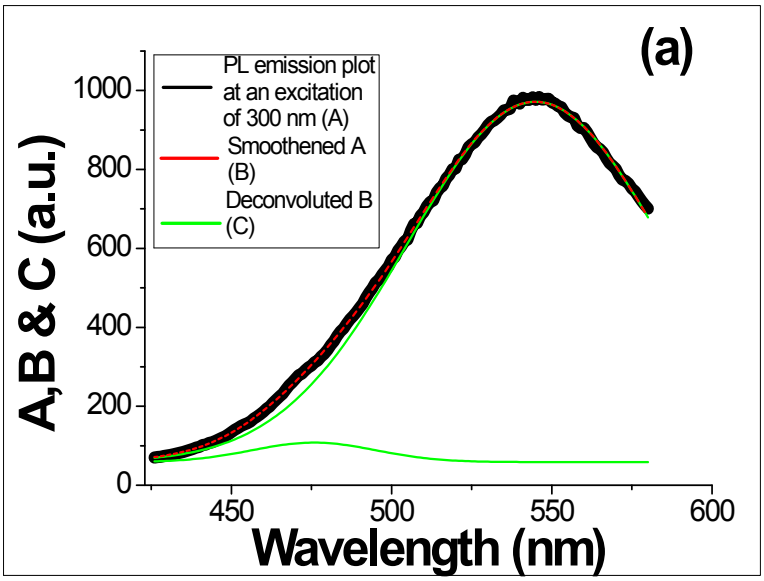


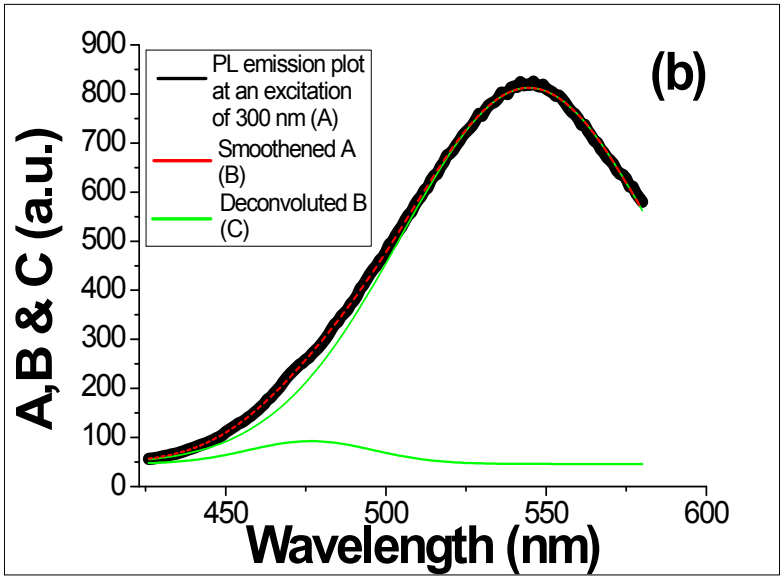


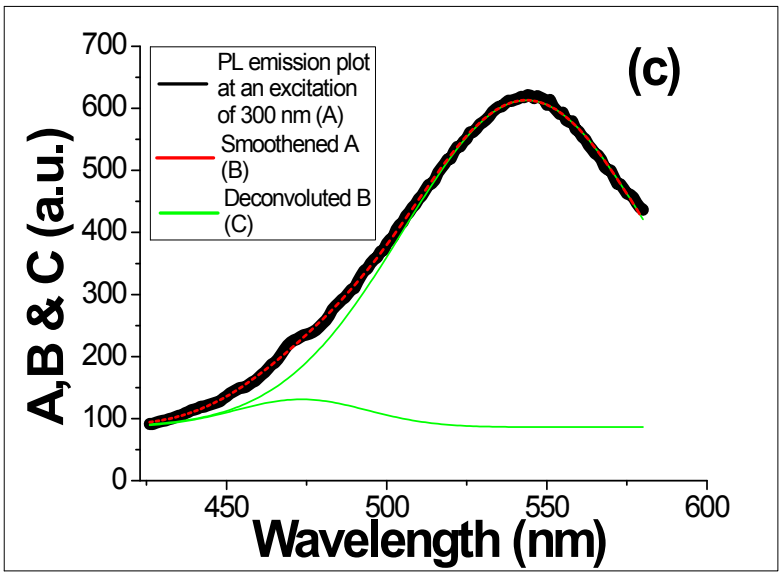

**S-7(B):** Configuration - coordinate diagram is generally used to describe the emission and absorption processes in solids. Here, the ground and excited electronic states, involved in the emission or absorption phenomenon, are described by classical quantum mechanical oscillators having quantum energy ħω[1] i.e. the emission centres can have their own set of vibrational energy states which is $E_0$ + nħω, where n is an integer and $E_0$ represents the ground state energy. Thus, their energy minima are displaced due to lattice vibration in the configuration coordinates.[2] Therefore the broad emission spectra is consisted of various emission energy ranging from $E_T = E_D - (E0 + n\hbar\omega)$, where $E_D$ represents the energy corresponding to higher energy states. In fact, theoretical calculation predicts that the maximum of the emission typically occurs at an excited state for which n ~ Huang – Rhys "S" factor. The significance of S is that it represents the strength of the electron-phonon interaction and it is calculated theoretically from half-width of the emission spectrum according to the following relation: [3, 4]

$$FWHM = 4(ln2)^{\frac{1}{2}}(kTS\hbar\omega)^{\frac{1}{2}}$$

On the otherhand, within the multi-phonon nonradiative, nonradiative relaxations of excited electrons are mediated by the excitation and emission of phonons and the corresponding rate ($k_{nr}$) is given by the following relation (3, 4):

$$k_{nr} = \frac{2\pi}{\hbar}[V_{ab}(R)]^2 exp[-S(2\acute{\gamma})]I_p\left(2S[\acute{\gamma}(\acute{\gamma}+1)]^{\frac{1}{2}}\right)[\acute{\gamma}(\acute{\gamma}+1)]^{\frac{p}{2}}$$

where $\acute{\gamma}$ is the Bose thermal occupation of phonon mode ħω, p is the exothermicity expressed as integral number of vibrational quanta, $I_p$ is a modified Bessel function. For further details please refer to Ref. 5.

**S - 8**: Decay plot of the PL emissions of ZQD, ZCF1, ZCF2 powders excited at 4.1 eV

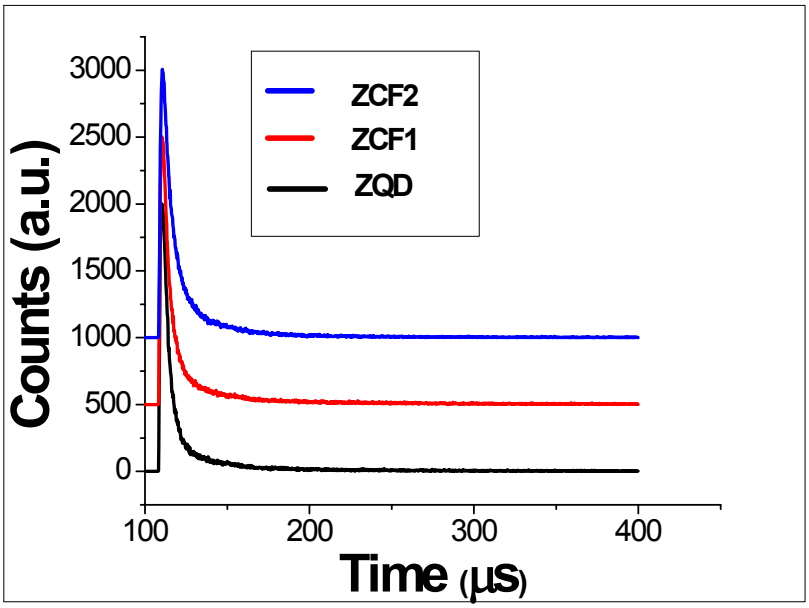


**S-9**: Time resolved PL data for ZnO QD

| Sample. Code | $\tau_1$ (μs) | $\tau_2$(μs) | $\tau_3$(μs) | $\tau_{avg}$(μs) | $B_1$ | $B_2$ | $B_3$ | Goodness of fit (χ) | intensity of PL w.r.t. : | | |
|---|---|---|---|---|---|---|---|---|---|---|---|
| | | | | | | | | | $\tau_1$ | $\tau_2$ | $\tau_3$ |
| ZQD | 3.99 | 22.01 | 112.7 | 26.00 | 2109.459 | 233.199 | 21.048 | 1.212 | 90 .0 | 9.80 | 0.2 |
| ZCF1 | 4.20 | 19.63 | 88.59 | 26.72 | 1988.201 | 290.611 | 41.823 | 1.135 | 85.7 | 12.5 | 1.8 |
| ZCF2 | 5.19 | 19.37 | 57.74 | 18.33 | 1744.029 | 401.471 | 48.782 | 1.088 | 79.5 | 18.3 | 2.2 |

**S-10**: Standard deviation of the fitted data of S-9

| Sample. Code | Standard deviation in $\tau_1$ ($10^{-2}$μs) | Standard deviation in $\tau_2$(μs) | Standard deviation in $\tau_3$ (μs) | Standard deviation in $B_1$ | Standard deviation in $B_2$ | Standard deviation in $B_3$ |
|---|---|---|---|---|---|---|
| ZQD | 5.42 | 1.11 | 27.05 | 18.52 | 8.63 | 4.11 |
| ZCF1 | 7.13 | 1.10 | 10.34 | 20.45 | 13.88 | 5.81 |
| ZCF2 | 1.17 | 1.28 | 7.16 | 27.85 | 21.04 | 14.04 |

**S- 11:** Justification for assigning $\tau_1$ and $\tau_2$ to nonradiative and radiative recombination:

Defect sites act as a source of non-radiative recombination centre i.e. samples with large defect concentration possesses higher decay probability of photo-generated charge carriers via nonradiative decay path rather than radiative decay path.[6] Here, we are examining the decay process of green emission that originates due to electronic transition between singly charged oxygen vacancy ($V_o^{\cdot}$) to zinc vacancy ($V_{Zn}$) sites i.e. we are considering decay process involving defect sites. Thus non-radiative decay is ascribed to be predominant here. If we compare the proportion of the decay processes corresponding to $\tau_1$ and $\tau_2$, it may be observed that percentage of the decay process corresponding to $\tau_1$ is very high i.e. decay process involving $\tau_1$ may be attributed to be non-radiative in nature. As discussed in the manuscript, the defect sites that causes the transition are deep level defect sites, thus we have ascribed them as shallow trapped electrons and shallow trapped holes. The effect of electron - phonon interaction is also observed from the variation of $A_1$(2LO)/$A_1$(LO). It decreases with increasing time, same trend is observed for FWHM of emission spectra.

References:


1. D.W. Cooke, B.L. Bennett, K.J. McClellan, J.M. Roper and M.T. Whittaker, *J. Appl. Phys.* 2000, 87, 7793.
2. F. Ciccacci, S. Selci, G. Chiarotti and P. Chiaradia, *Phys. Rev. Lett*, 1986, 56, 2411.
3. J. Shi, J. Chen, Z. Feng, T. Chen, X. Wang, P. Ying and C. Li, *J. Phys. Chem. B*, 2006, 110 25612.
4. Huang K., *Prog. Phys*. 1981, 1, 31.
5. *Jortner, J. J. Chem. Phys. 1976, 64, 4860*.
6. Kin Mun Wong, Yaoguo Fang, André Devaux, Liaoyong Wen, Jian Huang, Luisa De Cola and Yong Lei, *Nanoscale*, 3 (2011) 4830.